

Study of inherited thrombocytopenia resulting from mutations in *ETV6* or *RUNX1* using a human pluripotent stem cell model

Sara Borst,^{1,2} Catriana C. Nations,^{1,2} Joshua G. Klein,² Giulia Pavani,² Jean Ann Maguire,² Rodney M. Camire,^{2,3} Michael W. Drazer,⁴ Lucy A. Godley,⁴ Deborah L. French,^{2,5} Mortimer Poncz,³ and Paul Gadue^{2,5,*}

¹Department of Cell and Molecular Biology, University of Pennsylvania Perelman School of Medicine, Philadelphia, PA 19104, USA

²Center for Cellular and Molecular Therapeutics, Children's Hospital of Philadelphia, CTRB 5012, 3501 Civic Center Boulevard, Philadelphia, PA 19104, USA

³Department of Pediatrics, University of Pennsylvania Perelman School of Medicine and Children's Hospital of Philadelphia, Philadelphia, PA 19104, USA

⁴Section of Hematology/Oncology, Departments of Medicine and Human Genetics, The University of Chicago, Chicago, IL 60637, USA

⁵Department of Pathology and Laboratory Medicine, University of Pennsylvania Perelman School of Medicine and Children's Hospital of Philadelphia, Philadelphia, PA 19104, USA

*Correspondence: gaduep@email.chop.edu

<https://doi.org/10.1016/j.stemcr.2021.04.013>

SUMMARY

Inherited thrombocytopenia results in low platelet counts and increased bleeding. Subsets of these patients have monoallelic germline mutations in *ETV6* or *RUNX1* and a heightened risk of developing hematologic malignancies. Utilizing CRISPR-Cas9, we compared the *in vitro* phenotype of hematopoietic progenitor cells and megakaryocytes derived from induced pluripotent stem cell (iPSC) lines harboring mutations in either *ETV6* or *RUNX1*. Both mutant lines display phenotypes consistent with a platelet-bleeding disorder. Surprisingly, these cellular phenotypes were largely distinct. The *ETV6*-mutant iPSCs yield more hematopoietic progenitor cells and megakaryocytes, but the megakaryocytes are immature and less responsive to agonist stimulation. On the contrary, *RUNX1*-mutant iPSCs yield fewer hematopoietic progenitor cells and megakaryocytes, but the megakaryocytes are more responsive to agonist stimulation. However, both mutant iPSC lines display defects in proplatelet formation. Our work highlights that, while patients harboring germline *ETV6* or *RUNX1* mutations have similar clinical phenotypes, the molecular mechanisms may be distinct.

INTRODUCTION

Inherited thrombocytopenia (IT), caused by mutations in a variety of genes, is a genetic bleeding disorder resulting in low blood platelet counts. A subset of these patients harbor monoallelic germline mutations in the transcription factors *ETV6* or *RUNX1* (Savoia et al., 2017). Patients with monoallelic germline mutations in either of these genes phenocopy one another in terms of platelet defects and heightened hematologic malignancy predisposition; however, the disease pathology is not well understood (Dowton et al., 1985). One reason for this lack of understanding is the need for appropriate model systems. Mouse models have been utilized to study IT with risk of malignancy, but they fail to fully recapitulate the human disease phenotype. Specifically, mice heterozygous for *ETV6* have unperturbed hematopoiesis, whereas *RUNX1*-haploinsufficient mice have minimal thrombocytopenia (~15% reduction in platelet count) and do not develop leukemia, even with secondary hits (De Braekeleer et al., 2012; Hock et al., 2004; Sakurai et al., 2014; Sood et al., 2010).

Induced pluripotent stem cells (iPSCs) have proven to be a suitable model system to study developmental genetic disorders (Cherry and Daley, 2013). iPSC technology also allows for the generation of unlimited quantities of cells, which is important when studying disorders with limited patient population size and/or key samples. In addition,

patient-derived iPSCs can be genetically modified via CRISPR-Cas9 to yield isogenic control iPSC lines, which is critical when using human samples due to the large variation found in the human population. Genome-engineered iPSCs allow for detailed analysis of pathogenic mutations on the development of a disease-relevant cell type, such as the megakaryocyte (MK) (Musunuru, 2013).

Although the first case of IT with heightened risk of acute myeloid leukemia was described in 1978, heterozygous germline *RUNX1* mutations were not confirmed to be the cause until 1999 (Luddy et al., 1978; Song et al., 1999). *RUNX1* has since been studied extensively in megakaryopoiesis. In recent years, iPSC technology has been utilized to characterize the *in vitro* phenotype of iPSCs harboring *RUNX1* mutations (Antony-Debré et al., 2015; Connelly et al., 2014; Iizuka et al., 2015; Sakurai et al., 2014). These studies consistently highlight a defect in MK differentiation from hematopoietic progenitor cells (HPCs). However, an HPC phenotype is not always noted. More recently, mutations effecting *ETV6* have also been found to result in IT with predisposition for hematologic malignancy, mainly B cell acute lymphoblastic leukemia (Zhang et al., 2015). Since this discovery in 2015, studies in HeLa and primary human CD34⁺ cells show a defect in yielding large, proplatelet-forming *ETV6*-haploinsufficient MKs (Noetzli et al., 2015; Poggi et al., 2017; Zhang et al., 2015). To date, no *ETV6*-mutant patient-derived iPSC studies have been reported.

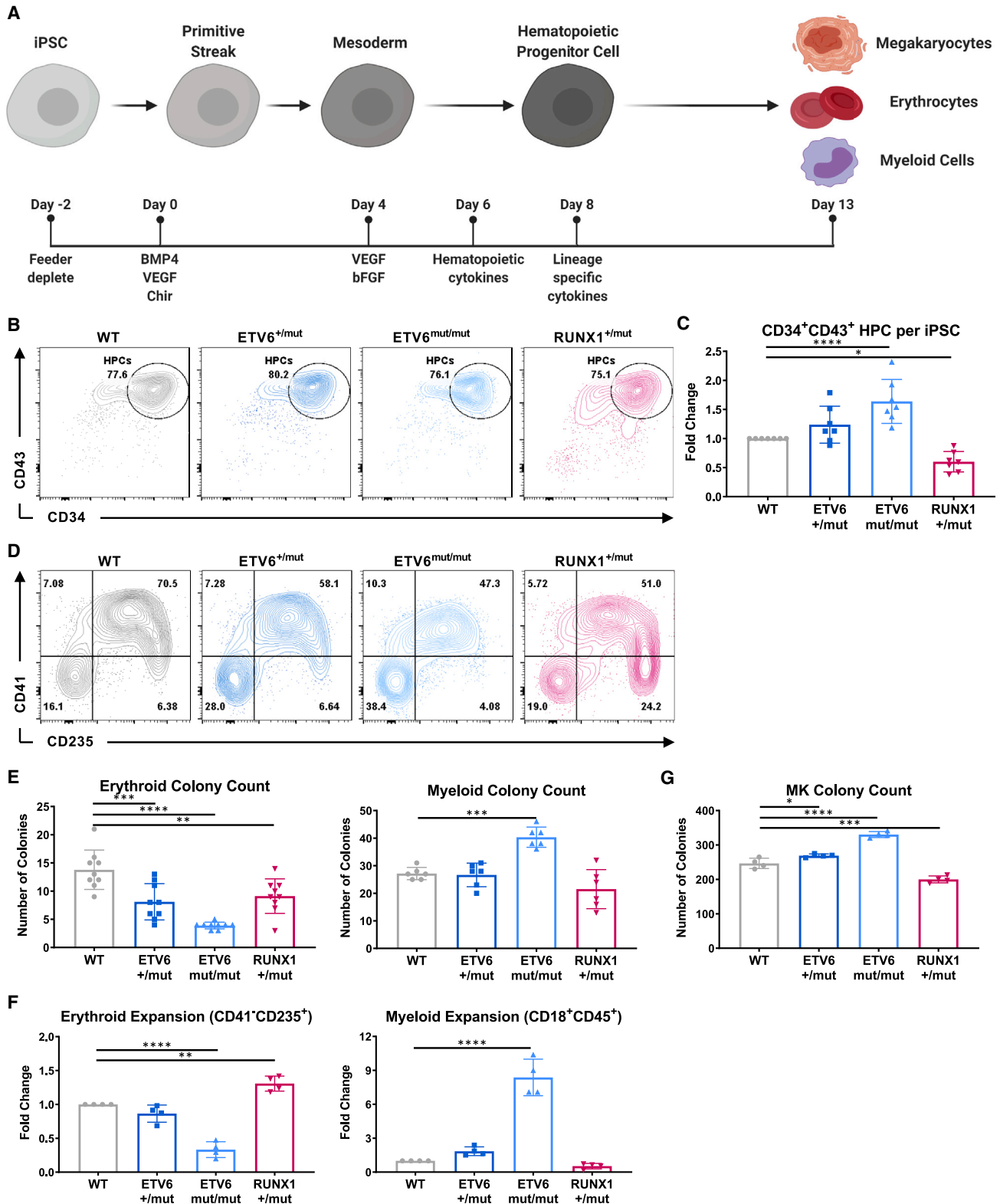


Figure 1. ETV6 and RUNX1 mutations reveal disparate lineage potentials in CHOPWT6 isogenic iPSC lines

(A) Schematic of adherent hematopoietic differentiation protocol.

(B) Representative flow profiles of HPCs.

(legend continued on next page)



In this study, we investigated the mechanism of IT caused by monoallelic mutations in the transcription factors *ETV6* or *RUNX1*. Although this disease has two parts—thrombocytopenia and hematologic malignancy—we focused our studies on the thrombocytopenia aspect as a more tractable endpoint. We found disparate phenotypes between the *ETV6*-mutant and *RUNX1*-mutant iPSC lines, although each mutant displayed distinct phenotypes consistent with thrombocytopenia. These studies highlight that pathogenic mutations may lead to the same phenotype in different ways, which can ultimately affect therapeutic treatment options.

RESULTS AND DISCUSSION

Generation and characterization of isogenic iPSC lines

To examine the role of *ETV6* and *RUNX1* in HPC and MK development, two different sets of iPSC lines were used: (1) patient-derived iPSCs harboring monoallelic germline *ETV6* or *RUNX1* mutations and (2) a wild-type (WT) iPSC line with the *ETV6* or *RUNX1* patient mutations introduced (Figures S1A–S1D and S2A–S2D). The latter system allowed for investigation of the pathogenic effects of these mutations in a common genetic background (CHOPWT6) (Somers et al., 2010). The *ETV6* patient mutation affects DNA binding without impacting dimerization, potentially acting as a dominant-negative (family B, Zhang et al., 2015). Western blot of the *ETV6*^{mut/mut} line showed little *ETV6* expression, suggesting that the mutation leads to protein instability (Figure S1F). The *RUNX1* patient was described previously as having a splice acceptor site mutation that results in haploinsufficiency (pedigree 3, Song et al., 1999). To introduce the patient mutations in the WT iPSC line and correct the mutation in the patient lines, CRISPR-Cas9 technology was used (Figures S1D and S2D) (Maguire et al., 2019). The gRNAs were designed near the patient mutations of interest (Figures S1A and S2A; Table S1), and clones expressing either heterozygous or homozygous mutations were confirmed by sequencing (Figures S1C and S2C). The WT isogenic set of iPSC lines are the main focus of these studies, while the patient-derived iPSC lines and isogenic corrected lines are used for validation in a second genetic background.

To establish the kinetics of *ETV6* or *RUNX1* expression during blood cell development, mRNA and protein expression were examined during the differentiation of iPSCs to HPCs and MKs. *ETV6* mRNA is expressed at low levels in undifferentiated iPSCs, whereas *RUNX1* mRNA is undetectable. Transcript levels of both *ETV6* and *RUNX1* increased significantly at the HPC and MK stages of differentiation (Figure S1E). Protein expression of *ETV6* suggests that the patient mutation affects protein production and/or stability (Figure S1F). The *RUNX1* splice defect was confirmed using reverse transcriptase PCR, demonstrating aberrant splicing at a downstream cryptic splice acceptor site (Figure S1G).

ETV6 and *RUNX1* mutations reveal disparate effects on blood differentiation

To determine the effect of these mutations on blood cell development, the iPSC lines were differentiated using a previously described protocol (Figure 1A) (Mills et al., 2014). The HPCs were isolated as single cells on day 8 of differentiation and analyzed by flow cytometry for CD34 and CD43 expression: CD34 is an early HPC marker, whereas CD43 is a pan-hematopoietic cell surface marker. We observed similar HPC flow profiles for all genotypes, but there was significantly fewer CD34⁺CD43⁺ HPCs in the *RUNX1*^{+/-mut} iPSC line compared with the WT, consistent with previous publications (Figures 1B and 1C) (Antony-Debré et al., 2015; Sakurai et al., 2014). In contrast, the yield of *ETV6*^{+/-mut} CD34⁺CD43⁺ HPCs was not significantly different when compared with the WT, while the *ETV6*^{mut/mut} line generated significantly more HPCs (Figure 1C).

Next, the lineage biases of these HPCs were analyzed by flow cytometry and colony assays. Cells were co-stained for cell surface expression of CD41 and CD235, markers for MK and erythroid commitment, respectively, whereas myeloid precursors were included within the population of double-negative cells within the CD34⁺CD43⁺ HPC population (Paluru et al., 2014; Vodyanik et al., 2005). Both the *ETV6*^{+/-mut} and *ETV6*^{mut/mut} HPCs were biased toward double-negative CD41⁻CD235⁻ cells, whereas the *RUNX1*^{+/-mut} HPCs were biased toward CD235⁺ cells when compared with the WT (Figure 1D). Colony assays confirmed these findings. The *ETV6*^{mut/mut} HPCs gave rise to more myeloid colonies and fewer erythroid colonies, whereas the *ETV6*^{+/-mut} lines gave rise to fewer erythroid colonies (Figure 1E).

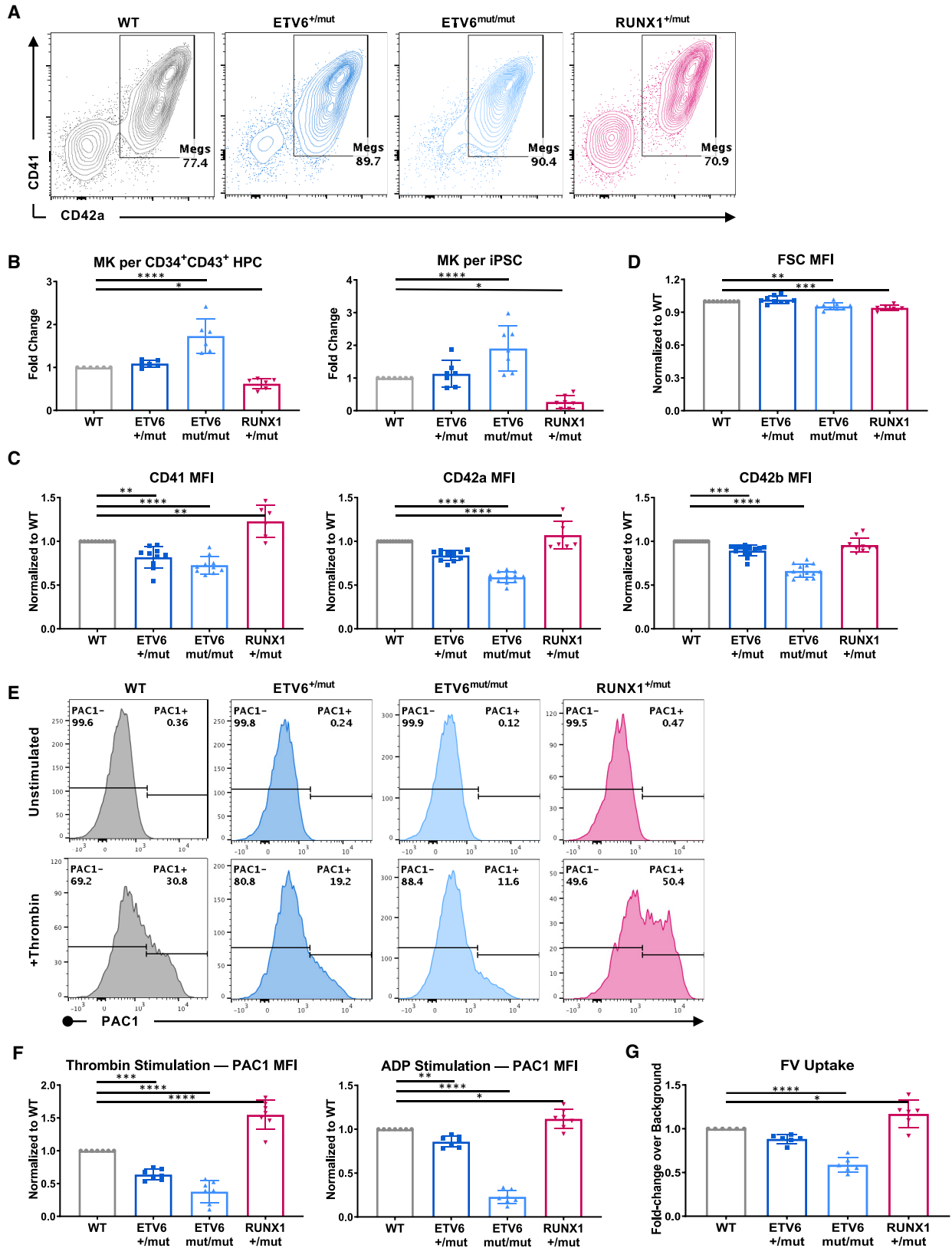
(C) Quantification of fold change in CD34⁺CD43⁺ HPCs per iPSC plated on day -2; normalized to WT. N = 7.

(D) Representative flow profiles of CD34⁺CD43⁺ HPC lineage biases: erythroid is CD41⁻CD235⁺, myeloid is CD41⁻CD235⁻.

(E) Quantification of number of erythroid (left) and myeloid (right) colonies after 12–14 days in methylcellulose-based medium. N = 9 for erythroid and N = 6 for myeloid.

(F) Quantification of erythroid (left) and CD18⁺CD45⁺ myeloid (right) cells after 5 days of culture; normalized to WT. N = 4.

(G) Quantification of number of MK colonies after 12 days in collagen-based medium. N = 4. For all statistical analyses, N indicates independent experiments. *p < 0.05, **p < 0.01, ***p < 0.001, ****p < 0.0001 in this and all subsequent figures.



(legend on next page)



Although the $RUNX1^{+/mut}$ HPCs gave rise to fewer erythroid colonies (Figure 1E), they were generally larger in size when compared with the WT. Culturing these HPCs in erythroid or myeloid liquid expansion conditions also supported these data: the $ETV6^{mut/mut}$ HPCs generated more myeloid cells, whereas the $RUNX1^{+/mut}$ HPCs generated more erythroid cells (Figure 1F). The MK potential of the HPCs was analyzed using the megacult colony assay. The $ETV6^{mut/mut}$ HPCs generated more MK colonies, whereas $RUNX1^{+/mut}$ HPCs generated fewer MK colonies (Figure 1G). These differences were confirmed using isogenic pairs of iPSC lines in a second genetic background for each (Figures S3A–S3E).

Contrasting MK phenotypes in $ETV6$ - and $RUNX1$ -mutant iPSC lines

To analyze the MK phenotype, $CD34^+CD43^+$ HPCs were cultured in medium containing thrombopoietin (TPO) and stem cell factor (SCF). By flow cytometry, all of the lines generated populations of $CD41^+CD42a^+$ MKs (Figure 2A). However, when calculating MK yield per input $CD34^+CD43^+$ HPCs, major differences were observed: the $ETV6^{mut/mut}$ HPCs generated more MKs (Figure 2B, left). In contrast, the $RUNX1^{+/mut}$ HPCs generated fewer MKs (Figure 2B, left). This same phenomenon was observed when calculating MK yield per input iPSC (Figure 2B, right). To determine if these differences were reflective of maturation defects, the expression of various receptors was analyzed during MK maturation using flow cytometry. The expression of $CD41$ (αIIb), an early marker of MK generation (Mitjavila-Garcia et al., 2002), was decreased on $ETV6^{+/mut}$ and $ETV6^{mut/mut}$ MKs but increased on $RUNX1^{+/mut}$ MKs (Figure 2C). The expression of $CD42a$ (GPIX) and $CD42b$ (GPIIb), both later markers of MK maturation (Nishikii et al., 2015), were decreased on $ETV6^{+/mut}$ and $ETV6^{mut/mut}$ MKs, whereas $CD42a$ was increased on $RUNX1^{+/mut}$ MKs (Figure 2C). Despite increased expression on $RUNX1^{+/mut}$ MKs, these MKs were slightly smaller in size, suggesting that receptor

expression was not correlated with surface area on these cells (Figure 2D). $ETV6^{mut/mut}$ MKs were also smaller compared with the WT iPSC line. These data suggest that the $ETV6$ mutant lines generated increased numbers of MKs with abnormal maturation marker expression, whereas the $RUNX1$ mutant line generated decreased numbers of MKs with normal maturation marker expression. These findings were consistent in a second genetic background (Figures S4A–S4C).

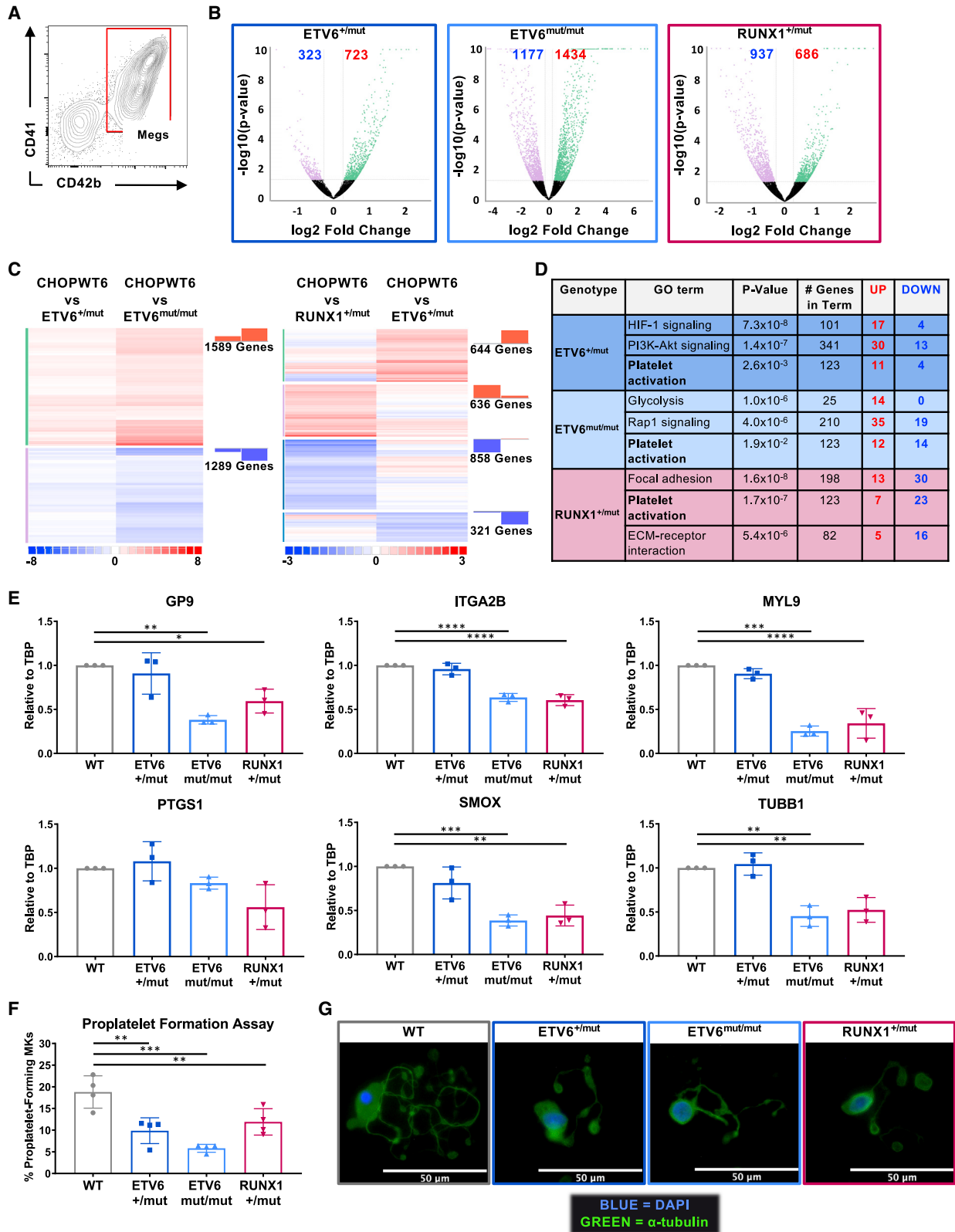
$ETV6$ -mutant MKs are less responsive to agonists than $RUNX1$ -mutant MKs

To test MK functionality, the responsiveness of MKs to stimulation by various agonists was analyzed. Activation with thrombin or adenosine 5'-diphosphate sodium salt (ADP) results in a conformational change in surface $\alpha IIb\beta 3$ receptors, thus enabling the binding of the conformation-specific monoclonal antibody, PAC1 (Shattil et al., 1985, 1987). All MKs showed no basal PAC1 binding, demonstrating no spontaneous pre-activation of these cells in culture (Figure 2E, top). Upon thrombin stimulation, ~30% of WT MKs responded to agonist stimulation (Figure 2E, bottom). This percentage was decreased to an average of ~15% for $ETV6^{mut/mut}$ MKs, but significantly increased to ~50% for $RUNX1^{+/mut}$ MKs (Figure 2E, bottom). Responsiveness was the same for both thrombin and ADP (Figure 2F).

Another assay measuring MK function is uptake of coagulation factor V (FV). We previously demonstrated that the uptake of fluorescently labeled FV positively correlated with MK maturation (Ivanciu et al., 2014; Sim et al., 2017). The uptake of FV by $ETV6^{mut/mut}$ MKs was decreased when compared with the WT, whereas the uptake of FV by $RUNX1^{+/mut}$ MKs was increased (Figure 2G). These data suggest that, although $ETV6^{mut/mut}$ MKs may be increased in number, they are less mature and responsive, whereas the $RUNX1^{+/mut}$ MKs were decreased in number, but appeared to be fully mature and more responsive when compared with the WT MKs. These phenotypes are

Figure 2. Disparate MK phenotypes in $ETV6$ - and $RUNX1$ -mutant CHOPWT6 iPSC lines

- (A) Representative flow profiles of $CD41^+CD42a^+$ MKs.
- (B) Quantification of MKs per $CD34^+CD43^+$ HPC (left) and per iPSC plated on day -2 (right) after 5 days of culture; normalized to WT. $N = 6$.
- (C) Quantification of mean fluorescence intensity (MFI) of MK markers after 5 days of MK culture; normalized to WT. For $CD41$ (left): $N = 10$ for WT, $ETV6^{+/mut}$, and $ETV6^{mut/mut}$; $N = 6$ for $RUNX1^{+/mut}$. For $CD42a$ (middle): $N = 12$ for WT, $ETV6^{+/mut}$, and $ETV6^{mut/mut}$; $N = 8$ for $RUNX1^{+/mut}$. For $CD42b$ (right): $N = 14$ for WT, $ETV6^{+/mut}$, and $ETV6^{mut/mut}$; $N = 10$ for $RUNX1^{+/mut}$.
- (D) Quantification of MK size after 5 days of culture via forward-scatter area (FSC) MFI; normalized to WT. $N = 9$ for WT, $ETV6^{+/mut}$ and $ETV6^{mut/mut}$; $n = 6$ for $RUNX1^{+/mut}$.
- (E) Representative flow histograms of PAC1 binding in unstimulated MKs (top) and thrombin stimulated MKs (0.1 U, bottom) after 6 days of MK culture.
- (F) Quantification of PAC1 MFI after stimulation with thrombin (left) or ADP (right) after 6 days of culture; fold change normalized to WT. $N = 7$.
- (G) Quantification of FV uptake over background in day 5 MKs; fold change normalized to WT. $N = 6$. For all statistical analyses, N indicates independent experiments.



(legend on next page)



consistent with disease, but suggestive of distinct mechanisms. All of these findings were similar in the second genetic background (Figures S4D and S4E).

RNA sequencing analysis of purified MKs and aberrant proplatelet signaling

To probe the molecular mechanism for these differences, genome-wide gene expression was performed on purified CD41⁺CD42b⁺ MKs from all four genotypes using RNA sequencing (Figure 3A). Comparing the mutant MKs with the WT and representing the data as volcano plots, ETV6^{+/-mut} MKs had 323 downregulated genes and 723 upregulated genes, which increased dramatically in number when the second allele of ETV6 was mutated (1,177 and 1,434, respectively) (Figures 3B and S4F). Compared with the WT, RUNX1^{+/-mut} MKs had 937 downregulated genes and 686 upregulated genes (Figures 3B and S4F). These data fit with ETV6 acting predominantly as a transcriptional repressor, and RUNX1 being a transcriptional activator (Noetzli et al., 2015; Rasighaemi et al., 2015; Topka et al., 2015; Zhang et al., 2015).

We compared differences in gene expression between the various genotypes via a meta-analysis that utilizes an unsupervised clustering algorithm to bin genes into distinct subpopulations. When comparing the WT with both the ETV6^{+/-mut} and ETV6^{mut/mut} MKs, a trend was observed in up- and downregulated genes, with a higher degree of dysregulation in the ETV6^{mut/mut} MKs compared with the ETV6^{+/-mut} MKs (Figure 3C, left). In contrast, when RUNX1^{+/-mut} and ETV6^{+/-mut} MKs were compared with the WT, there was minimal overlap in dysregulated genes, with genes up or down in one mutant line but not the other (Figure 3C, right). Overall, these data are in line with our other findings that show disparate phenotypes and support the idea that ETV6 and RUNX1 haploinsufficiency leads to MK defects via distinct mechanisms.

Despite the differences in gene expression between ETV6- and RUNX1-mutant MKs, Kyoto Encyclopedia of Genes and Genomes pathway analysis revealed platelet

activation and cancer-related signaling pathways as the top gene ontology terms for both genotypes (Figure 3D; Table S3). Examination of mRNA expression of a human platelet gene set (Rowley et al., 2011) showed a similar degree of downregulation in genes crucial for proplatelet formation and platelet function between ETV6^{mut/mut} and RUNX1^{+/-mut} MKs (Figure 3E; Table S4). Finally, the proplatelet-forming abilities of these mutant-MK populations were examined through adhesion to a fibrinogen substrate. The efficiency and complexity of the resultant proplatelet structures were significantly reduced in ETV6- and RUNX1-mutant MKs compared with the isogenic control (Figures 3F and 3G). These findings suggest that the genes dysregulated as a result of mutations in ETV6 or RUNX1 may share some common pathways to ultimately disrupt proplatelet formation and thrombopoiesis, in spite of the overall differences.

These experimental studies and RNA sequencing data show that the molecular mechanism driving at least the thrombocytopenia differs in patients with monoallelic mutations in ETV6 or RUNX1. However, despite differing phenotypes, the end result is the same: for ETV6-mutants, there are more, but less responsive MKs, and for RUNX1 mutants, there are fewer, but more responsive MKs. Both ETV6- and RUNX1-mutant MKs are deficient in proplatelet formation, and would therefore give rise to fewer platelets compared with the isogenic control (Figure 4).

EXPERIMENTAL PROCEDURES

Differentiation of iPSCs into HPCs and MKs

iPSCs were differentiated into HPCs as described previously (Mills et al., 2014). HPCs were isolated as single cells and differentiated toward MK lineage at 37°C with 5% CO₂. HPCs were cultured in serum-free defined (SFD) medium supplemented with TPO (50 ng/mL) (R&D) and SCF (25 ng/mL) (R&D) for 5–6 days, with fresh medium added on top every 2 days. SFD medium is defined as: 750 mL homemade Iscove's modified Dulbecco's medium (Sigma), 250 mL HAMS/F12 (Corning), 5 mL N2 supplement (Gibco), 10 mL B27 supplement (Gibco), 5 mL 10% bovine serum

Figure 3. RNA sequencing of purified CHOPWT6 isogenic MKs show aberrant proplatelet signaling

- Gating strategy for MK purification sort before RNA isolation.
- Volcano plots showing differential gene expression compared with WT. Each dot represents a gene, with the coloring of the dot reflecting the clustering information for each gene: black dots are genes that do not pass the filter parameters; green dots are genes that are upregulated compared with WT; purple dots are genes that are downregulated compared with WT. The number of up- and downregulated genes are noted in red and blue, respectively.
- Meta-analysis heatmap independently comparing WT with ETV6^{+/-mut} and ETV6^{mut/mut} (left), and WT with RUNX1^{+/-mut} and ETV6^{+/-mut} (right). The overall trend in gene expression for each cluster is depicted above the total number of genes in each cluster.
- Top gene ontology terms from Kyoto Encyclopedia of Genes and Genomes pathway analysis.
- Graphs validating platelet gene expression from MK RNA sequencing data via qPCR. N = 3.
- Graph quantifying the percent proplatelet-forming CD41⁺ MKs out of total adhered CD41⁺ MKs. N = 4.
- Representative immunofluorescence images of proplatelet-forming MKs. Blue, DAPI; green, α -tubulin. For all statistical analyses, N indicates independent experiments.

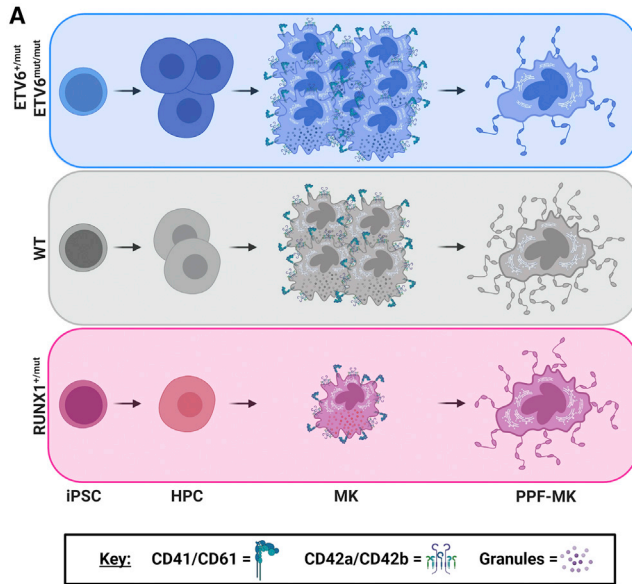


Figure 4. Model

(A) In comparison with the WT isogenic control, *ETV6*-mutant iPSCs generate more HPCs that yield higher numbers of less-responsive MKs, whereas *RUNX1*^{+/mut} iPSCs generate fewer HPCs that yield fewer numbers of more responsive MKs. Both *ETV6*- and *RUNX1*-mutant MKs display defects in the ability to form proplatelet extensions, suggesting that platelet production and release will be poor in comparison with the WT isogenic control. Schematic was created using BioRender software.

albumin (BSA) in PBS (Sigma), 2 mM glutamine, and 1 × penicillin/streptomycin.

MK activation

MKs were suspended in Tyrode's salt solution (Sigma) with 0.1% BSA to a final concentration of 1 × 10⁶ cells/mL. Cells were stained with anti-CD42a, anti-CD42b, and PAC1 antibodies (see Table S2) and stimulated with thrombin (0.01–0.1 U final) (Sigma) or ADP (1–10 μM final) (Sigma) in a total volume of 100 μL for 10 min at room temperature followed by incubation on ice, in the dark.

Pulse labeling of MKs with coagulation FV

MKs were pulse-labeled with FV by incubating with 200 nM of a previously described FV variant tagged with Alexa 488 for 1 h at 37°C (Ivanciu et al., 2014).

Proplatelet formation assay

HPCs were cultured in StemSpan Serum-Free Expansion Medium II (SFEM II) (STEMCELL Technologies) with TPO (50 ng/mL) and SCF (25 ng/mL) for 5–7 days at 37°C with 5% CO₂ to promote MK differentiation. In 12-well tissue culture-treated plates, sterile glass coverslips (EMS) were washed with PBS and coated with 100 μg/mL fibrinogen (Millipore) in PBS for 2 h. Coverslips were blocked with 1% BSA for 1 h, and removed 15 min before MK seeding. MKs were resuspended in seeding medium (SFEM II with TPO [50 ng/mL]) at

a concentration of 2,000 MKs/μL and 1 × 10⁵ MKs were seeded on the center of each coverslip. MKs were left to adhere for 1 h at 37°C before flooding with 500 μL of seeding medium per well and incubating for an additional 24 h. Coverslips were fixed with 4% paraformaldehyde (Thermo Scientific) in PBS for 20 min at room temperature, washed 3 × with PBS and left in 1 mL PBS for imaging. Images were taken at 20 × in random locations and proplatelet-forming MKs were counted using Fiji software.

Statistical analysis

Statistical analysis and figure generation were performed using GraphPad Prism 6 software. The results are represented as mean ± standard error of the mean. Ordinary one-way ANOVA with multiple comparisons were used with correction for multiple comparisons using statistical hypothesis testing performed using Tukey. In figures *p < 0.05, **p < 0.01, ***p < 0.001, ****p < 0.0001.

Data and code availability

The accession number for the RNA-seq data reported in this paper is GEO: GSE168326.

SUPPLEMENTAL INFORMATION

Supplemental information can be found online at <https://doi.org/10.1016/j.stemcr.2021.04.013>.

AUTHOR CONTRIBUTIONS

S.B. conceptualized and performed the described studies, interpreted data, and prepared the manuscript and figures. C.C.N., J.G.K., and G.P. performed the proplatelet formation experiments. J.A.M. reprogrammed the patient-derived iPSC lines and assisted in manuscript review. R.M.C. provided the fluorescently labeled FV and assisted in manuscript review and editing. M.W.D. and L.A.G. provided patient sample access and assisted in manuscript review and editing. M.P. assisted in the overall conceptualization, data interpretation, and manuscript review and editing. D.L.F. and P.G. provided overall scientific guidance and manuscript preparation.

DECLARATION OF INTERESTS

The authors declare no competing interests.

ACKNOWLEDGMENTS

These studies were supported by NIH grants T32-GM007229 (to S.B.), T32-DK007780 (to S.B.), F31-HL140774 (to S.B.), R01-HL130698 (to M.P., D.L.F., and PG), U01-HL134696 (to D.L.F. and P.G.), a Leukemia and Lymphoma Society Translational Research Award (to L.A.G.), and a RUNX1 Research Program grant in an association with the Alex Lemonade Foundation (to M.P., D.L.F., and P.G.).

Received: September 25, 2020

Revised: April 20, 2021

Accepted: April 21, 2021

Published: May 20, 2021



REFERENCES

- Antony-Debré, I., Manchev, V.T., Balayn, N., Bluteau, D., Tomowiak, C., Legrand, C., Langlois, T., Bawa, O., Tosca, L., Tachdjian, G., et al. (2015). Level of RUNX1 activity is critical for leukemic predisposition but not for thrombocytopenia. *Blood* *125*, 930–940.
- De Braekeleer, E., Douet-Guilbert, N., Morel, F., Le Bris, M.J., Basinko, A., and De Braekeleer, M. (2012). ETV6 fusion genes in hematological malignancies: a review. *Leuk. Res.* *36*, 945–961.
- Cherry, A.B.C., and Daley, G.Q. (2013). Reprogrammed cells for disease modeling and regenerative medicine. *Annu. Rev. Med.* *64*, 277–290.
- Connelly, J.P., Kwon, E.M., Gao, Y., Trivedi, N.S., Elkahloun, A.G., Horwitz, M.S., Cheng, L., and Liu, P.P. (2014). Targeted correction of RUNX1 mutation in FPD patient-specific induced pluripotent stem cells rescues megakaryopoietic defects. *Blood* *124*, 1926–1930.
- Downton, S.B., Beardsley, D., Jamison, D., Blattner, S., and Li, F.P. (1985). Studies of a familial platelet disorder. *Blood* *65*, 557–563.
- Hock, H., Meade, E., Medeiros, S., Schindler, J.W., Valk, P.J.M., Fujiwara, Y., and Orkin, S.H. (2004). Tel/Etv6 is an essential and selective regulator of adult hematopoietic stem cell survival. *Genes Dev.* *18*, 2336–2341.
- Iizuka, H., Kagoya, Y., Kataoka, K., Yoshimi, A., Miyauchi, M., Taoka, K., Kumano, K., Yamamoto, T., Hotta, A., Arai, S., et al. (2015). Targeted gene correction of RUNX1 in induced pluripotent stem cells derived from familial platelet disorder with propensity to myeloid malignancy restores normal megakaryopoiesis. *Exp. Hematol.* *43*, 849–857.
- Ivanciu, L., Krishnaswamy, S., and Camire, R.M. (2014). New insights into the spatiotemporal localization of prothrombinase in vivo. *Blood* *124*, 1705–1714.
- Luddy, R.E., Champion, L.A.A., and Schwartz, A.D. (1978). A fatal myeloproliferative syndrome in a family with thrombocytopenia and platelet dysfunction. *Cancer* *41*, 1959–1963.
- Maguire, J.A., Cardenas-Diaz, F.L., Gadue, P., and French, D.L. (2019). Highly efficient CRISPR/Cas9 mediated genome editing in human pluripotent stem cells. *Curr. Protoc. Stem Cell Biol.* *48*, 1–22.
- Mills, J.A., Paluru, P., Weiss, M.J., Gadue, P., and French, D.L. (2014). Hematopoietic differentiation of pluripotent stem cells in culture. *Methods Mol. Biol.* *1185*, 181–194.
- Mitjavila-Garcia, M.T., Cailleret, M., Godin, I., Nogueira, M.M., Cohen-Solal, K., Schiavon, V., Lecluse, Y., Le Pesteur, F., Lagrue, A.H., and Vainchenker, W. (2002). Expression of CD41 on hematopoietic progenitors derived from embryonic hematopoietic cells. *Development* *129*, 2003–2013.
- Musunuru, K. (2013). Genome editing of human pluripotent stem cells to generate human cellular disease models. *Dis. Model. Mech.* *6*, 896–904.
- Nishikii, H., Kanazawa, Y., Umamoto, T., Goltsev, Y., Matsuzaki, Y., Matsushita, K., Yamato, M., Nolan, G.P., Negrin, R., and Chiba, S. (2015). Unipotent megakaryopoietic pathway bridging hematopoietic stem cells and mature megakaryocytes. *Stem Cells* *33*, 2196–2207.
- Noetzli, L., Lo, R.W., Lee-Sherick, A.B., Callaghan, M., Noris, P., Savoia, A., Rajpurkar, M., Jones, K., Gowan, K., Balduini, C.L., et al. (2015). Germline mutations in ETV6 are associated with thrombocytopenia, red cell macrocytosis and predisposition to lymphoblastic leukemia. *Nat. Genet.* *47*, 535–538.
- Paluru, P., Hudock, K.M., Cheng, X., Mills, J.A., Ying, L., Galvão, A.M., Lu, L., Tiyaboonchai, A., Sim, X., Sullivan, S.K., et al. (2014). The negative impact of wnt signaling on megakaryocyte and primitive erythroid progenitors derived from human embryonic stem cells. *Stem Cell Res.* *12*, 441–451.
- Poggi, M., Canault, M., Favier, M., Turro, E., Saultier, P., Ghalloussi, D., Baccini, V., Vidal, L., Mezzapesa, A., Chelghoum, N., et al. (2017). Germline variants in ETV6 underlie reduced platelet formation, platelet dysfunction and increased levels of circulating CD34+ progenitors. *Haematologica* *102*, 282–294.
- Rasighaemi, P., Liongue, C., Onnebo, S.M.N., and Ward, A.C. (2015). Functional analysis of truncated forms of ETV6. *Br. J. Haematol.* *171*, 658–662.
- Rowley, J.W., Oler, A.J., Tolley, N.D., Hunter, B.N., Low, E.N., Nix, D.A., Yost, C.C., Zimmerman, G.A., and Weyrich, A.S. (2011). Genome-wide RNA-seq analysis of human and mouse platelet transcriptomes. *Blood* *118*, e101–e111.
- Sakurai, M., Kunimoto, H., Watanabe, N., Fukuchi, Y., Yuasa, S., Yamazaki, S., Nishimura, T., Sadahira, K., Fukuda, K., Okano, H., et al. (2014). Impaired hematopoietic differentiation of RUNX1-mutated induced pluripotent stem cells derived from FPD/AML patients. *Leukemia* *28*, 2344–2354.
- Savoia, A., Gnan, C., and Faleschini, M. (2017). Inherited thrombocytopenias with predisposition the hematological malignancies. *Annu. Rev. Hematol. Oncol.* *1*, 1–7.
- Shattil, S.J., Hoxie, J.A., Cunningham, M., and Brass, L.F. (1985). Changes in the platelet membrane glycoprotein IIb/IIIa complex during platelet activation. *J. Biol. Chem.* *260*, 11107–11114.
- Shattil, S.J., Cunningham, M., and Hoxie, J.A. (1987). Detection of activated platelets in whole blood using activation-dependent monoclonal antibodies and flow cytometry. *Blood* *70*, 307–315.
- Sim, X., Jarocho, D., Hayes, V., Hanby, H.A., Marks, M.S., Camire, R.M., French, D.L., Poncz, M., and Gadue, P. (2017). Identifying and enriching platelet-producing human stem cell-derived megakaryocytes using factor V uptake. *Blood* *130*, 192–204.
- Somers, A., Jean, J.C., Sommer, C.A., Omari, A., Ford, C.C., Mills, J.A., Ying, L., Gianotti, A.S., Jean, J.M., Smith, B.W., et al. (2010). Generation of transgene-free lung disease-specific human induced pluripotent stem cells using a single excisable lentiviral stem cell cassette. *Stem Cells* *28*, 1728–1740.
- Song, W.-J., Sullivan, M.G., Legare, R.D., Hutchings, S., Tan, X., Kufirin, D., Ratajczak, J., Resende, I.C., Haworth, C., Hock, R., et al. (1999). Haploinsufficiency of CBFA2 causes familial thrombocytopenia with propensity to develop acute myelogenous leukaemia. *Nat. Genet.* *23*, 166–175.



Sood, R., English, M.A., Belete, C.L., Jin, H., Bishop, K., Haskins, R., McKinney, M.C., Chahal, J., Weinstein, B.M., Wen, Z., et al. (2010). Development of multilineage adult hematopoiesis in the zebrafish with a *runx1* truncation mutation. *Blood* *115*, 2806–2809.

Topka, S., Vijai, J., Walsh, M.F., Jacobs, L., Maria, A., Villano, D., Gaddam, P., Wu, G., McGee, R.B., Quinn, E., et al. (2015). Germline *ETV6* mutations confer susceptibility to acute lymphoblastic leukemia and thrombocytopenia. *PLoS Genet.* *11*, 1–14.

Vodyanik, M.A., Bork, J.A., Thomson, J.A., and Slukvin, I.I. (2005). Human embryonic stem cell-derived CD34+ cells: efficient production in the coculture with OP9 stromal cells and analysis of lymphohematopoietic potential. *Blood* *105*, 617–626.

Zhang, M.Y., Churpek, J.E., Keel, S.B., Walsh, T., Lee, M.K., Loeb, K.R., Gulsuner, S., Pritchard, C.C., Sanchez-Bonilla, M., Delrow, J.J., et al. (2015). Germline *ETV6* mutations in familial thrombocytopenia and hematologic malignancy. *Nat. Genet.* *47*, 180–185.